Sub-fF 130 nm MOS Varactor Characterization using 6 . 8 GHz Interferometry-based Reflectometer

Pietro Maris Ferreira, Cora Donche, Ambroise Delalin, Thomas Quémerais, Daniel Gloria, Tuami Lasri, Gilles Dambrine, Christophe Gaquière

Sub-fF 130 nm MOS Varactor Characterization using 6.8 GHz Interferometry-based Reflectometer

Pietro Maris Ferreira, *Member, IEEE*, Cora Donche, Ambroise Delalin, Thomas Quémerais, Daniel Gloria, Tuami Lasri, Gilles Dambrine, *Senior Member, IEEE*, and Christophe Gaquière

***Abstract*—Nanometer-scaled communication devices for microwave and millimeter wave applications motivated innovative techniques in modeling and characterization. In this letter, an interferometry-based reflectometer (IBR), comprising Vector Network Analyser (VNA) and commercial devices, is implemented. Using sub-fF 130 nm thick-oxide accumulation MOS varactors from ST Microelectronics, IBR and VNA measurements are compared to a silicon-based model. A capacitance from 0.9 to 1.6 fF around 6.8 GHz is estimated. IBR demonstrates a root-mean-squared (RMS) error related to silicon-based model of 60 aF, while VNA has 70 aF in its best case. The mean accuracy is estimated at 40 aF and 11 aF respectively for VNA best case and IBR in C-V measurements This letter demonstrates that IBR solution has smaller RMS error and better accuracy for C-V measurements than VNA.**

***Index Terms*—Interferometry-based reflectometer, sub-fF MOS varactor, high-impedance microwave and millimeter wave instrumentation**

I. Introduction

Microwave and millimeter wave wireless communications have strongly motivated the development of new instrumentation techniques. Since voltage controlled oscillator (VCO) employs accumulation-mode MOS varactor for frequency tuning, precise capacitance-voltage (C-V) estimation is required. He et al. [1] and Cho et al. [2] have designed millimeter wave VCOs using varactors of hundreds of femtofarads in 130 nm technology. To increase oscillation frequency, a solution is to design sub-femtofarad (sub-fF) capacitors and inductors with few hundreds of picohenries. However, an accurate measurement of sub-fF C-V variation should be verified for better estimation of VCO tuning slope (voltage-to-frequency).

Reflection-coefficient measurements using vector network analyzer (VNA) is the most accepted technique to characterize capacitors at microwave and millimeter wave frequencies. Nevertheless as VNA has its best sensitivity for impedances close to its normalized impedance (i.e. 50 Ω) [3], it is not accurate enough while measuring high-impedance variation. In [4], Happy et al. have formalized this challenge, demonstrating that VNA impedance uncertainty drastically increases in millimeter wave frequency band.

Recent studies have explored alternative instrumentation techniques to increase accuracy and stability. Moertelmaier et al. [5] have demonstrated interferometry-based C-V curves for 1 to 20 GHz range. Dargent et al. have highlighted reflectometer measurements from 0.1 to 10 fF MOS capacitors at 3.5 GHz [6]. Both publications are interested in scanning microwave applications using atomic-force microscopy. Happy et al. have explored interferometry-based techniques and compared carbon nano-tubes measurements using a standard VNA, and a Wheatstone bridge [4].

Varactors RF measurements by using an interferometry-based technique have already been studied by Debroucke et al. [7]. The preliminary IBR measurements of MOS varacators achieved in Debroucke's study have been obtained by a relatively complex architecture that includes mixers and amplifiers. Compared to this previous study, this work addresses this challenge by using a simpler architecture. In addition, measurements of RMS error and mean accuracy are presented to achieve a formal comparison of IBR and VNA tools.

In this letter, an IBR associating a VNA and on the shelves passive devices is implemented. IBR measurement results are validated for a sub-fF 130 nm MOS varactors around 6.8 GHz. To demonstrate IBR benefits, IBR and VNA measurements are compared to a silicon-based model. RMS error and mean accuracy are evaluated. This letter innovates in sub-fF capacitance characterization in microwave and millimeter wave frequency, opening the way to an important increase of VCO frequency.

II. Interferometry-Based Reflectometer

A. Test-Bench Implementation

Interferometry principle is to achieve a destructive interference between reference device (REF) and a tuner (TUN) reflection waves. Thus, electromagnetic wave results in a nil residue of reflection coefficient (Γ_{nil}) as [8]

$$\Gamma_{nil} = \frac{\Gamma_{TUN} + \Gamma_{REF}}{2}, \tag{1}$$

where $|\Gamma_{TUN}|$ calibration (nulling process) is accomplished using an attenuator; and $\angle\,\Gamma_{TUN}$ is obtained using coaxial delay lines. To control instrumentation frequency, IBR implementation would require a precise and reconfigurable delay device, not included in this work.

Figure 1 illustrates the selected architecture to implement an IBR. Based on Dargent et al. work [6], reflectometer architecture is simplified to reduce costs and to be suited for RF microprobe. The VNA is an Agilent PNA (E8363B), which is capable to source and receive RF signals from 10 MHz to 40 GHz. Source signal is split by a 3 dB power divider (PD) being RADIALL (R463805). *L* signal is further attenuated by NARDA 791FM, which has attenuation fine-control from 0 to

P. M. Ferreira, is with GeePs, UMR CNRS 8507, CentraleSupélec - Campus Gif-sur-Yvette, France; email: maris@ieee.org. C. Donche, A. Delalin, T. Lasri, G. Dambrine and C. Gaquière are with IEMN, UMR CNRS 8520, Lille 1 Univ., France. T. Quémerais, and D. Gloria are with STMicroelectronics, 850 rue Jean Monnet 38926 Crolles, France.

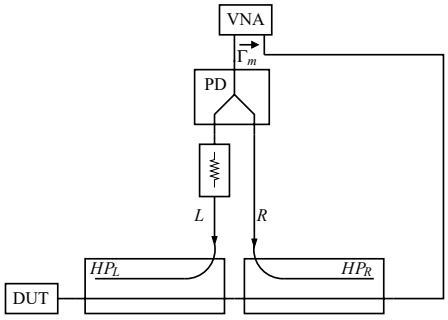

Figure 1. IBR block diagram: illustration.

37.5 dB. R signal is delayed in flexible coaxial cable. HP_L coupler combines the device-under-test (DUT) reflected wave with attenuated source wave. HP_R coupler combines DUT reflected wave with delayed source wave. Both devices are a HP 11691D having -20 dB coupling for a frequency range from 2 to 18 GHz. In this test bench, the DUT is a sub-fF MOS varactor integrated in BiCMOS130 nm ST Microelectronics technology. The DUT is measured using MPI Allstron GSG 125 RF microprobes, and biased in [-2.5, 2.5 V].

B. Instrumentation Protocol

Reflection coefficient measurement using IBR requires a calibration step. While calibrating IBR, a reference device is chosen (a 26 fF capacitor) replacing DUT in Figure 1. A destructive wave interference is carried out according to Equation (1). With this purpose, attenuator is adjusted, until $\Gamma_m \leq \Gamma_{nil}$ (specified as $\Gamma_{nil} = -65$ dB) is obtained. To guarantee stable calibration, the IBR employs VNA with an IF bandwidth of 30 Hz and a span of 1 MHz. Thus, IBR frequency resolution is improved and measurement time reduced. Finally, a working frequency ($f_{nil} \approx 6.8$ GHz) is established.

IBR is modeled using a traditional tracking error method

$$\Gamma_m = E_{11} + \frac{E_{21} \cdot E_{12} \Gamma_i}{1 - E_{22} \Gamma_i}, \tag{2}$$

where Γ_m is the measured reflection coefficient for a calibrated IBR [4]. To solve this model equation, transmission line capacitances (C_i being 26, 65, and 135 fF) from an ISS Cascade Microtech 101-190B LRM GSG 100-250 μm are measured at f_{nil} using calibrated IBR. Besides, theoretical reflection coefficients (Γ_i) are calculated and IBR tracking errors are found.

During measurement step, a DUT is connected and its Γ_m obtained. The DUT is a sub-fF MOS varactor biased from -2.5 V to 2.5 V with 100 mV step (51 points) at f_{nil}. To reduce measurements incertitude, the instrumentation protocol considers an average of five different C-V curve measurements. Using this instrumentation protocol, IBR's data acquisition takes place in 180 s. Without lifting and lowering RF microprobes between measurements, the instrumentation protocol also avoids placement errors.

III. VNA Reflection-Coefficient Measurement

To demonstrate IBR benefits, reflection-coefficient measurements of the DUT are performed using a VNA. An Agilent VNA (E8361A) is L2RM calibrated with IF bandwidth of 1 Hz. DUT capacitance (C_{DUT}) is estimated using the phase-shift ($\angle\Gamma_{DUT}$), being

$$C_{DUT} = \frac{-tan\left(\angle\Gamma_{DUT}/2\right)}{2\pi f_{min} Z_{VNA}}, \tag{3}$$

where $Z_{VNA} = 50\ \Omega$ [4]. To estimate uncertainty in VNA measurements, an average procedure was considered. First, VNA measurement incertitude is estimated using a single measurement (associated to VNA_1 results) at 6.8 GHz using a resonant approach in 1 MHz bandwidth to be consistent with IBR instrumentation protocol. VNA data acquisition is ended after 10 minutes. Five- (VNA_5) and twenty-averaged (VNA_{20}) measurement results were obtained. VNA_5 acquisition requires 30 minutes, and VNA_{20} acquisition needs 2 hours.

IV. 130 nm MOS varactor measurements

A. Silicon-Based Modelling

A T-cell model is used to consider varactor physical elements including substrate parameters. The silicon-based model developed by STMicroelectronics is scalable for all varactors dimensions: gate finger length (l), gate finger width (w), number of gate fingers (N) and the number of devices in parallel ($Mult$). MOS varactor capacitance (C_s) is given by the relationship

$$C_s = \frac{1}{\frac{1}{C_{ox}(w,N,l)} + \frac{1}{C_{sc}(w,N,l)}} + C_{metal}(w,N,l) + C_{peri}(w,N,l). \tag{4}$$

C_{metal} is metal-interconnection parasitic, dependent of the geometrical and physical dimensions of the varactor. C_{peri} is perimeter-fringe parasitic, mainly dependent on the varactor finger gate perimeter dimensions. The voltage dependent MOS capacitance is equivalent of semiconductor (C_{sc}) and oxide (C_{ox}) capacitances. Both C_{sc} and C_{ox} are based on the BSIM 4 compact model with specific ST Microelectonics fitting parameters [9]. This model enables to accurately simulate varactors behavior up to millimeter wave frequencies for all geometries. In this work, DUT sizing is $l = 0.13$ μm, $w = 1.5$ μm, $N = 1$, and $Mult = 1$.

B. IBR Calibration and Modelling

The IBR (see Figure 1) was calibrated according to the procedure described in Sec. II-B. The NARDA attenuator was configured for 1 dB attenuation to obtain the specified Γ_{nil}. Figure 2 shows the Γ_m of reference capacitor in calibration step (nulling process). The IBR achieves a $\Gamma_{nil} = -65.5$ dB at $f_{nil} = 6.824$ GHz. Reflectometer modelling is carried out and the tracking errors are calculated following Eq. (2).

C. IBR and VNA Measurements Comparison

Figure 3(a) presents sub-fF MOS varactor C-V curves comparing silicon-based model to IBR, and VNA averaged measurements. A RMS error (RMSE) is chosen as suitable figure-of-merit to compare C-V measurements to silicon-based model. Using

$$RMSE_i = \sqrt{mean\left(\left(C_i - C_{model}\right)^2\right)}, \tag{5}$$

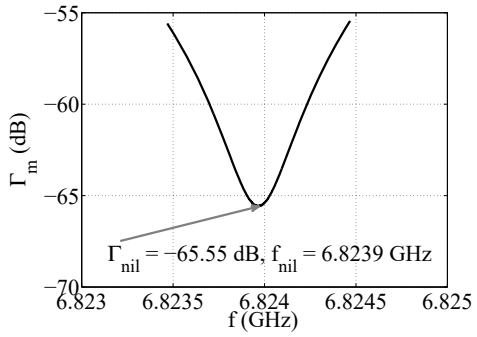

Figure 2. Reflection coefficient for 26 fF reference capacitor.

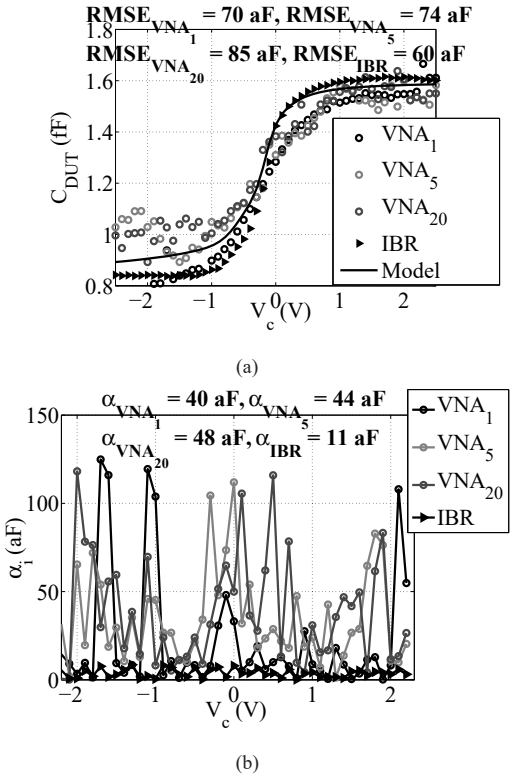

Figure 3. Sub-fF MOS varactor characterization: (a) C-V curves using silicon-based model, VNA, and IBR; (b) Measure accuracy for VNA, and IBR measurements.

$RMSE_{VNA_1}$, $RMSE_{VNA_5}$, $RMSE_{VNA_{20}}$ are found to be bigger than $RMSE_{IBR}$. This result experimentally exhibits the impedance mismatch stated in [4].

To estimate sub-fF C-V slope, a mean accuracy is chosen as figure-of-merit. Measured (ΔC_i) and silicon-based model (ΔC_{model}) C-V slopes are compared using

$$\alpha_i = \sqrt{mean\left(\left(\Delta C_i - \Delta C_{model}\right)^2\right)}. \quad (6)$$

Figure 3(b) clearly highlights that α_{IBR} C-V slope is more accurate than α_{VNA_1}, α_{VNA_5}, and $\alpha_{VNA_{20}}$.

VNA averaging procedure was tested to verify measurement uncertainty reduction. However, RMSE and α figures-of-merit demonstrated that uncertainty increases in VNA_5 and VNA_{20} results. In fact, the VNA protocol requires a non-negligible time to obtain C-V measurement (i.e. 10 min. for VNA_1, 30 min for VNA_5, and 2 h for VNA_{20}). Thus, VNA_{20} and VNA_5 are more sensitive to the drift induced by environmental noise which is not considered during VNA calibration. Therefore, averaged VNA measurements demonstrated a worse accuracy compared to non-averaged.

V. Conclusions

This letter presents an IBR tool associating VNA and on the shelves devices. Sub-fF 130 nm MOS varactors were characterized from 0.9 to 1.6 fF around 6.8 GHz. This work experimentally proves that IBR is capable to measure capacitance variations with a much better accuracy than VNA. While VNA measurements presented 40 aF of mean accuracy in best case, IBR mean accuracy presented 11 aF. Moreover, $RMSE_{IBR} = 60$ aF is smaller than what is found in VNA measurements (i.e. 70 aF in best case). IBR instrumentation opens the way to an important increase in VCO oscillation frequency by sub-fF varactors integration.

Acknowledgment

Authors would like to thank Dr. K. Haddadi for his suggestions to improve this letter. The project received funding from the French Government and the Regional Council. This work has benefited of the facilities of ExCELSiOR-Nanoscience Characterization Center.

References

[1] J. He, J. Li, D. Hou, Y.-z. Xiong, D. L. Yan, P. Khm, L. P. H. D. Vwdu, and H. G. X. Vj, "A 20-GHz VCO for PLL Synthesizer in 0 . 13- μ m BiCMOS," in *IEEE Proc. of RFIC*, 2012, pp. 231–233.

[2] L.-c. Cho, C. Lee, and S.-i. Liu, "A 1.2 V 37-38.5 GHz Eight-Phase Clock Generator in 0.13 um CMOS Technology," *IEEE J. Solid-State Circuits*, vol. 42, no. 6, pp. 1261–1270, 2007.

[3] H. P. Huber, I. Humer, M. Hochleitner, M. Fenner, M. Moertelmaier, C. Rankl, A. Imtiaz, T. M. Wallis, P. Hinterdorfer, P. Kabos, J. Smoliner, J. J. Kopanski, and F. Kienberger, "Calibrated nanoscale dopant profiling using a scanning microwave microscope," *J. Appl. Phys.*, vol. 014301, no. 111, 2012.

[4] H. Happy, K. Haddadi, D. Théron, T. Lasri, and G. Dambrine, "Measurement Techniques for RF Nanoelectronic Devices," *IEEE Microwave Magazine*, vol. 15, no. 1, pp. 30–39, 2014.

[5] M. Moertelmaier, H. P. Huber, C. Rankl, and F. Kienberger, "Ultramicroscopy Continuous capacitance - voltage spectroscopy mapping for scanning microwave microscopy," *Ultramicroscopy*, vol. 136, pp. 67–72, 2013.

[6] T. Dargent, K. Haddadi, T. Lasri, N. Clément, D. Ducatteau, B. Legrand, H. Tanbakuchi, and D. Theron, "An interferometric scanning microwave microscope and calibration method for sub-fF microwave measurements." *The Review of scientific instruments*, vol. 84, no. 12, p. 123705, Dec. 2013.

[7] R. Debroucke, D. Gloria, D. Ducatteau, D. Theron, H. Tanbakuchi, and C. Gaquiere, "attoF MOS Varactor RF Measurement VNA coupled with interferometer," in *77th ARFTG Microwave Measurement Conference*, 2011, pp. 2–3.

[8] K. Haddadi, H. Bakli, and T. Lasri, "Microwave Liquid Sensing Based on Interferometry and Microscopy Techniques," *Microwave Wireless Compon. Lett.*, vol. 22, no. 10, pp. 542–544, Oct. 2012.

[9] T. Quemerais, D. Gloria, D. Golanski, and S. Bouvot, "High-Q MOS Varactors for Millimeter-Wave Applications in CMOS 28 nm FDSOI," *IEEE Electron Devices Letter*, accepted.